Supporting Information

Polyelectrolyte-Based Physical Adhesive Hydrogels with Excellent Mechanical Strength for Biomedical Applications

Wenxiang Li,[1] Ruyan Feng,[2] Rensheng Wang,[1] Dan Li, [2] Wenwen Jiang,[1] Hanzhou Liu,[1] Zhenzhong Guo,[3, *] Michael J. Serpe,[4] Liang Hu[1, *]

1. State Key Laboratory of Radiation Medicine and Protection, School for Radiological and Interdisciplinary Sciences (RAD-X), Collaborative Innovation Center of Radiation Medicine of Jiangsu Higher Education Institutions and Jiangsu Provincial Key Laboratory of Radiation Medicine and Protection, Soochow University, Suzhou, Jiangsu, 215123, China

2. College of Chemistry, Chemical Engineering and Materials Science, Soochow University, Suzhou, Jiangsu, 215123, China

3. Hubei Province Key Laboratory of Occupational Hazard Identification and Control, Medical College, Wuhan University of Science and Technology, Wuhan, Hubei, 430065, China

4. Department of Chemistry, University of Alberta, Edmonton, AB, T6G 2G2, Canada

Zhenzhong Guo, E-mail: zhongbujueqi@hotmail.com

Liang Hu, E-mail:huliang@suda.edu.cn

1.

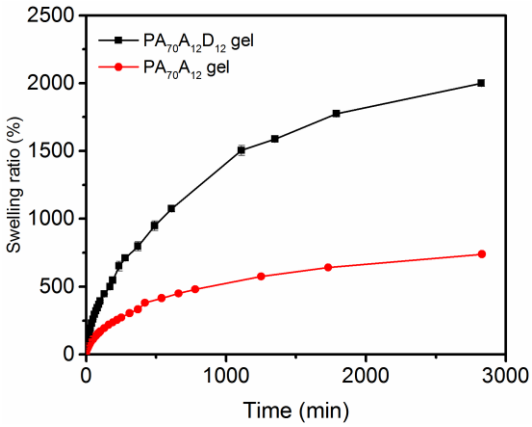

Figure S1. The swelling ratio of hydrogels at room temperature. Each data point in the average of 3 measurements, with the error bars showing the standard deviation.

2.

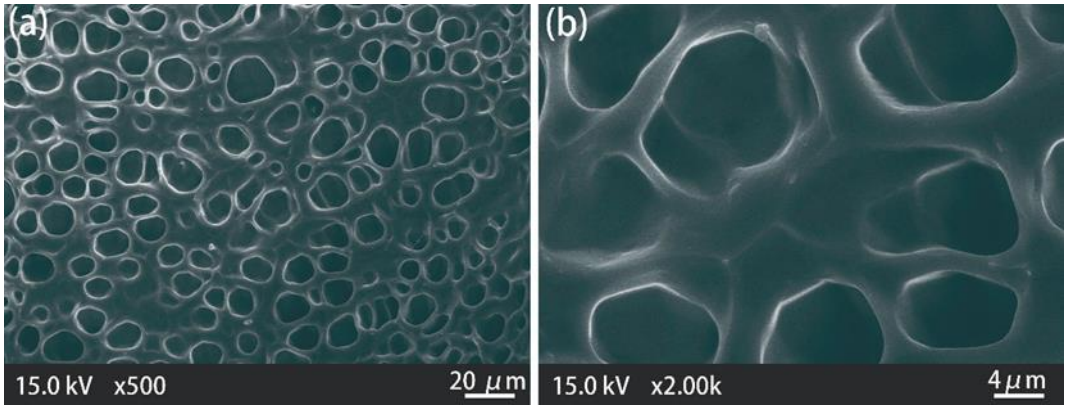

Figure S2. SEM images of the $PA_{70}A_{12}D_{12}$ hydrogel.

3.

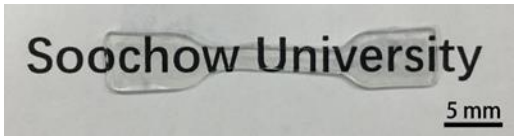

Figure S3. Photograph of a dumbbell shaped the $PA_{70}A_{12}D_{12}$ hydrogel (GB/T 1040-1992).

4.

Figure S4. Photographs of the $PA_{70}A_yD_z$ hydrogel with various content of ionic pairs.

5.

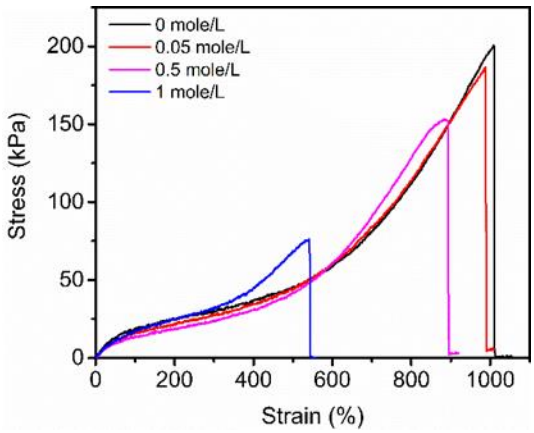

Figure S5. The tensile stress-strain curves of $PA_{70}A_{12}D_{12}$ hydrogels which were prepared through the precursor solution with various ionic strength.

6.

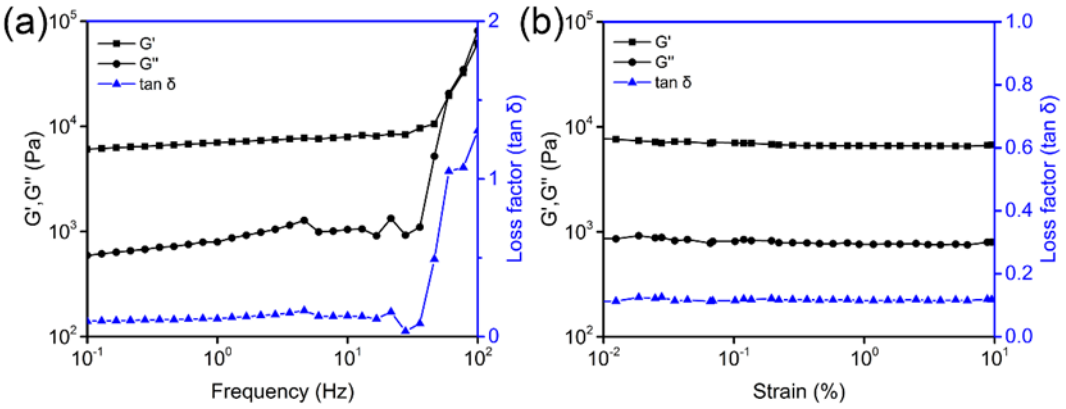

Figure S6. Dynamic mechanical properties of the $PA_{70}A_{12}D_{12}$ hydrogel. (a) Frequency-sweep and (b) strain-sweep measurments.

7.

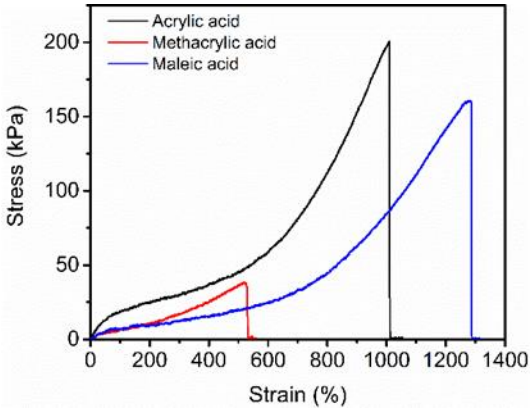

Figure S7. Stress-strain curves of hydrogels with different anionic reactive monomers, such as poly(AAm-*co*-methacrylic acid)/PDADMAC and poly(AAm-*co*-maleic acid)/PDADMAC hydrogels. Herein, both hydrogels were synthesized by using the same method as $PA_xA_yD_z$ hydrogels. Briefly, 12 mmole of methacrylic acid (or 6 mmole of maleic acid) was added to replace AAc (12 mmole).

8.

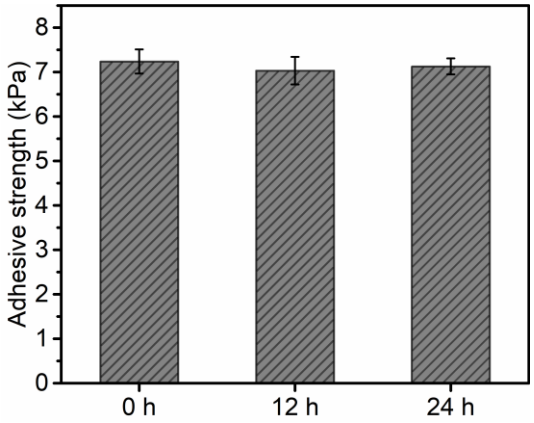

Figure S8. The adhesive strength of the hydrogel on PE substrates after different storing time. Each data point in the average of 3 measurements, with the error bars showing the standard deviation.

9.

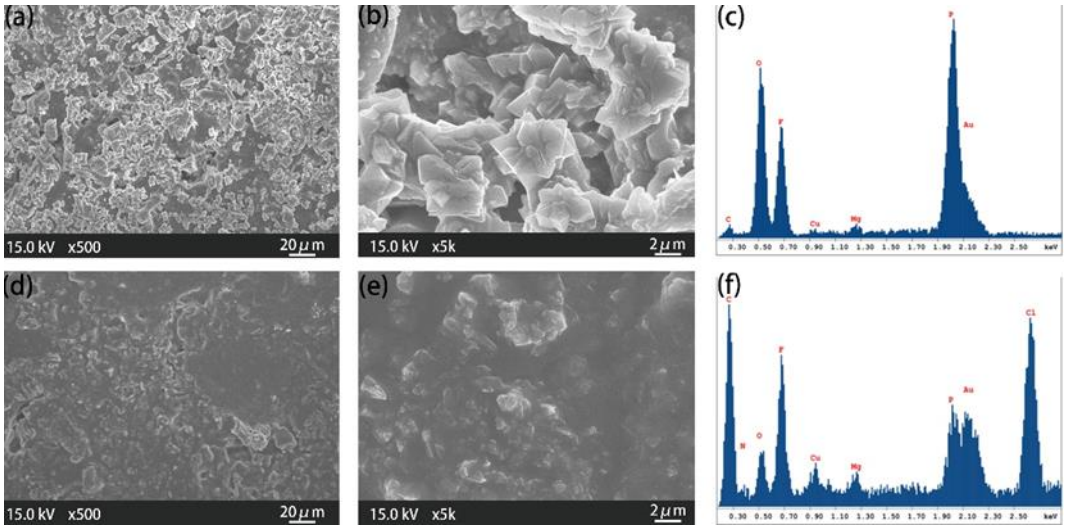

Figure S9. SEM EDX images and spectra of (a-c) pristine TLDs and (d-f) TLD-hydrogel hybrids.

10.

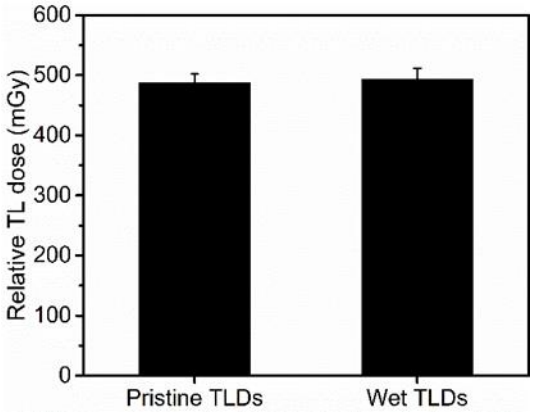

Figure S10. The effect of water on the relative TL doses for samples. Wet TLDs were prepared by immersing TLDs in DI water prior to the exposure to X-ray radiation. Each data point in the average of 3 measurements, with the error bars showing the standard deviation.

11.

When the incident angle is ~87°, the penetration of X-rays ($d_{X\text{-}ray}$) is ~ 2.5 mm *via* a simple geometric calculation. According to Figure S10, $D_{r(c3/c1)}$ should have detected ~328.691 mGy

(91.7% of $D_{r(c2)}$) if all TLDs have been located at the same SSD, which is higher than our detection. As a result, the lower the magnitudes of $D_{r(c1)}$ and $D_{r(c3)}$ is caused by the reduced SSD and increased incident angle in this case.

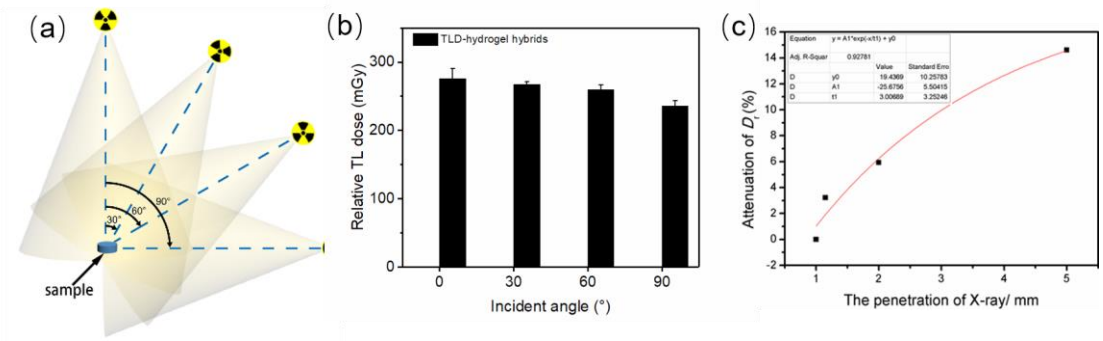

Figure S11. The relative TL dose of samples vary as a function of (a, b) incident angles at 100 mGy min^{-1} under X-ray. Accumulated dose was 1000 mGy. Each data point in the average of > 3 measurements, with the error bars showing the standard deviation. (c) The attenuation of D_r as a function of the penetration depth of X-rays. The penetration of X-rays was depended on the incident angles of X-rays and the geometry size of the TLDs.

12.

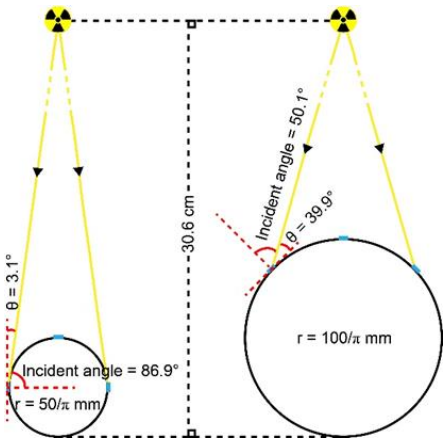

Figure S12. The geometry of TLD (shown in blue)-hydrogel hybrids deposited on curved surfaces with different radii.

Table S1. Mechanical properties and structural parameters of $PA_xA_{12}D_{12}$ hydrogels.

hydrogels	E (kPa)	σ_f (kPa)	ε_f (%)	U (kJ m^{-3})	τ (kPa)	N^* (mol m^{-3})
$PA_{40}A_{12}D_{12}$	3.8±0.6	47.6±8.9	654±23	100.0±11.2	7.8±0.6	1.8
$PA_{50}A_{12}D_{12}$	9.6±1.9	113.3±16.4	817±16	285.9±28.8	12.7±1.3	2.9
$PA_{60}A_{12}D_{12}$	19.9±2.1	174.2±12.8	900±27	489.5±24.3	17.1±1.0	3.9
$PA_{70}A_{12}D_{12}$	26.9±2.7	200.2±14.4	1013±54	679.4±31.2	25±3.7	5.7
$PA_{80}A_{12}D_{12}$	36.5±3.1	214.8±21.4	934±35	705.2±33.0	28.8±2.1	6.6
$PA_{90}A_{12}D_{12}$	44.1±4.1	232.4±19.4	845±11	671.1±25.1	33.8±1.9	7.8

Table S2. Mechanical properties and structural parameters of $PA_{70}A_yD_z$ hydrogels with varying AAc concentration (y=z).

PDADMAC	E (kPa)	σ_f (kPa)	ε_f (%)	U (kJ m^{-3})	τ (kPa)	N^* (mol·m^{-3})
2	11.1±2.6	29.6±4.3	2120±62	347.5±24.2	6.2±1.0	1.4
7	21.4±1.9	157.9±11.2	1380±45	732.2±28.1	13.2±1.7	3
12	26.9±2	200.2±14.4	1013±54	679.4±31.2	18.6±2.1	4.3
17	39±2.2	150±17.1	704±48	395.7±19.2	21.6±1.5	5.3
22	43.3±3.1	128.0±9.5	623±29	340.9±24.1	25.0±2.7	5.7

Table S3. Mechanical properties and structural parameters of $PA_{70}A_yD_z$ hydrogels with varying mole ratio of anions to cations (y:z).

y:z	E (kPa)	σ_f (kPa)	ε_f (%)	U (kJ m^{-3})	τ (kPa)	N^* (mol m^{-3})
1:9	54.4±7.9	435±34	14.9±2.8	114.0±37.1	22.4±1.2	5.1
3:7	135.1±12.4	713±42	20.1±2.4	325.7±28.9	22.6±0.8	5.2
5:5	200.2±14.4	1013±54	26.9±2	679.4±31.2	25±1.6	5.7
7:3	182.6±16.8	1097±27	23.7±1.9	643.1±42.1	17.8±2.0	4.1
9:1	60.6±9.7	1839±82	22.1±0.7	433.0±33.5	10.3±1.5	2.4